6122 J. Med. Chem. 2010, 53, 6122–6128
DOI: 10.1021/jm100533p

Journal of Medicinal Chemistry Article

Identification and Characterization of Acidic Mammalian Chitinase Inhibitors

Derek C. Cole,*[,†,∥] Andrea M. Olland,*[,‡] Jaison Jacob,[‡,⊥] Jon Brooks,[§] Matthew G. Bursavich,[†,#] Robert Czerwinski,[†] Charlene DeClercq,[§] Mark Johnson,[‡] Diane Joseph-McCarthy,[†,▽] John W. Ellingboe,[†] Laura Lin,[‡] Pawel Nowak,[†] Ella Presman,[‡] James Strand,[‡] Amy Tam,[‡] Cara M. M. Williams,[§] Shihua Yao,[‡] Désirée H. H. Tsao,[‡] and Lori J. Fitz[§]

[†] *WorldWide Medicinal Chemistry: Inflammation & Immunology,* [‡] *Global BioTherapeutics Technologies, and* [§] *BioTherapeutics R&D Inflammation & Immunology, Pfizer Global Research & Development, 200 Cambridge Park Drive, Cambridge, Massachusetts 01240.* [∥] *Current Address: Takeda San Diego, 10410 Science Center Drive, San Diego, California 92121.* [⊥] *Current Address: Novartis Institutes for BioMedical Research, Inc., 250 Massachusetts Avenue, Cambridge, Massachusetts 02139.* [#] *Current Address: Myriad Pharmaceuticals, 320 Wakara Way, Salt Lake City, Utah 84108.* [▽] *Current Address: AstraZeneca R & D Boston, 35 Gatehouse Drive, Waltham, Massachusetts 02451*

Received May 4, 2010

Acidic mammalian chitinase (AMCase) is a member of the glycosyl hydrolase 18 family (EC 3.2.1.14) that has been implicated in the pathophysiology of allergic airway disease such as asthma. Small molecule inhibitors of AMCase were identified using a combination of high-throughput screening, fragment screening, and virtual screening techniques and characterized by enzyme inhibition and NMR and Biacore binding experiments. X-ray structures of the inhibitors in complex with AMCase revealed that the larger more potent HTS hits, e.g. 5-(4-(2-(4-bromophenoxy)ethyl)piperazine-1-yl)-1*H*-1,2,4-triazol-3-amine **1**, spanned from the active site pocket to a hydrophobic pocket. Smaller fragments identified by FBS occupy both these pockets independently and suggest potential strategies for linking fragments. Compound **1** is a 200 nM AMCase inhibitor which reduced AMCase enzymatic activity in the bronchoalveolar lavage fluid in allergen-challenged mice after oral dosing.

Introduction

Asthma's prevalence and mortality have been increasing worldwide, and the World Health Organization (WHO[a]) recognizes that asthma is a disease of major public health importance. Asthma is a chronic pulmonary disease caused by inhaled allergens and mediated by T-helper type 2 (Th2) cytokines including IL-4, IL-5, and IL-13.[1] AMCase, a member of glycosyl hydrolase 18 family,[2] is up-regulated in lung tissue of allergen challenged asthma patients and is elevated in lung macrophage cells from patients with fatal asthma.[3] AMCase is also up-regulated in lung tissue in several Th2 dependent mouse models of allergic pulmonary disease and is dependent on IL-13 signaling.[4,5] In a non chitin dependent allergic airway disease model, inhibition of AMCase by either the broad spectrum chitinase inhibitor methylallosamidin,[6,7] or an antibody specific to AMCase, ameliorate airway inflammation and hyperresponsiveness.[3] However, increased expression of AMCase is protective in a chitin dependent model of pulmonary inflammation.[8] To aid in identifying the role of AMCase in mouse models of allergic pulmonary disease and further validate AMCase as a target for human asthma, additional potent selective small molecule inhibitors are needed.

We previously reported the cloning, expression, and purification of human AMCase and development of a fluorescence-based substrate hydrolysis assay suitable for high-throughput screening (HTS).[9] The availability of highly pure protein allowed the crystallization and determination of high-resolution X-ray structures of AMCase in the apo form and in complex with the inhibitor methylallosamidin.[10] Thus, because of the novelty of the AMCase target and the availability of protein for biophysical and X-ray crystallographic studies, complementary screening techniques, including HTS, fragment-based screening (FBS) by NMR binding experiments, and virtual screening (VS) were employed to improve the opportunities of identifying attractive lead-like starting points for optimization.

Herein, we report the identification of AMCase inhibitors using these complementary techniques. In addition, HTS hits were characterized by NMR binding experiments and surface plasmon resonance (SPR) by Biacore was used to determine the kinetics of binding while X-ray crystallography was used to obtain structural information and guide optimization.

Results and Discussion

HTS is an important part of drug discovery at pharmaceutical and biotechnology companies, and the leads for many clinical candidates were identified through HTS.[11,12] Typically, hundreds of thousands to millions of compounds are screened at a single concentration using a suitable assay. Compounds which cause a statistically significant effect are retested at a single or multiple concentrations to confirm activity

*To whom correspondence should be addressed. Phone: +1-858-731-3534 (D.C.C.); +1-617-665-5044 (A.M.O.). E-mail: derek.cole@takedasd.com (D.C.C.); andrea.olland@pfizer.com (A.M.O.).

[a] Abbreviations: AMCase, acidic mammalian chitinase; FBS, fragment-based screening; HTS, high-throughput screening; LE, ligand efficiency; LLE, ligand-lipophilic efficiency; MM-PBSA, molecular mechanics-Poisson−Boltzmann surface area; STD, saturation transfer difference; SPR, surface plasmon resonance; Th2, T-helper type 2; VS, virtual screening; WHO, World Health Organization; HDM, house dust mite; CRA, cockroach allergen; BAL, bronchoalveolar lavage; Dex, dexamethasone.

 Published on Web 07/28/2010

and determine potency. Despite the success of HTS, the process is complex and expensive. Frequently, a large hit set is identified, which include real inhibitors as well as false positives, such as compounds that bind nonspecifically and compounds that interfere with the assay signal. The challenge is to prioritize the hit set to smaller numbers which may be fully characterized in lower throughput binding experiments without losing the best hits. Prioritization based on potency frequently leads to larger, less lead-like inhibitors, which have been shown to evolve frequently into drug candidates with undesirable physiochemical properties.[13] Strategies based on calculated properties, including ligand efficiency (LE) and ligand-lipophilic efficiency (LLE),[13,14] are more likely to lead to more lead-like hits with lower molecular weight and lipophilicity.

The AMCase HTS assay based on hydrolysis of the fluorescent-based substrate, 4-methylumbelliferyl-β-D-*N*,*N*′-diacetylchitobioside,[9] was used to screen a library of 446000 compounds at 10 μM concentration and identified 5257 compounds with $>14\%$ apparent inhibition. Reconfirmation resulted in 825 confirmed hits which were chemically triaged to remove any non-lead-like structures and give a set of 500 compounds, which were tested in a 15-point titration to determine the IC_{50} for AMCase and selectivity versus chitotriosidase.

In the past decade, the field of FBS has emerged and been successfully applied to several protein targets, leading to the identification of novel leads,[15,16] showing good complementarity to the HTS hits. FBS techniques typically screen hundreds to thousandss of low molecular weight compounds (typically MW $<$ 300 Da). This fragment universe is estimated at 1.6×10^6 molecules, and thus a larger portion of the chemical space can be explored with smaller libraries.[17] Fragments are likely to have fewer binding interactions with the protein, resulting in the expectation of weaker binding and thus are usually screened at higher concentration. However, these binding interactions are frequently more optimal and lead to the fragments having higher binding efficiency.[13] With the aid of structural information, fragment leads are frequently readily optimized, leading to high affinity inhibitors.[18,19] Many biophysical techniques have been used to detect direct binding of fragment libraries such as NMR,[20,21] SPR,[22,23] mass spectrometry,[24] and X-ray crystallography.[25]

NMR was used to screen the library consisting of 1045 fragments, using the saturation transfer difference (STD) experiment. The fragments were screened as mixtures of six compounds, and mixtures which demonstrated binding were deconvoluted by evaluating individual compound binding followed by competition experiments with methylallosamidin. A total of 15 compounds displayed significant STD signal ($>4\%$) indicating binding, and of these, 10 compounds, showed a substantial decrease in the STD signal with addition of methylallosamidin, suggesting that they bind in the active site of AMCase (for example, **3**, Figure 1). All of the FBS hits showed modest inhibitory activity in the AMCase assay e.g. **4** ($IC_{50} = 102$ μM), with the exception of a more potent fragment, **3** (AMCase $IC_{50} = 13$ μM). A substructure search based on **4** rapidly led to the 5-fold more potent analogue **5** (AMCase $IC_{50} = 22.5$ μM), indicating how in some cases the potency of weak fragment hits may be rapidly optimized.

VS using either structure-based and ligand-based methods can be employed separately or in combination[26] as a complementary approach to both HTS and FBS, expanding the scope of the overall screen and exploiting existing structural and ligand information.[27] For structure-based VS, typically hierarchical scoring schemes are utilized that allow databases

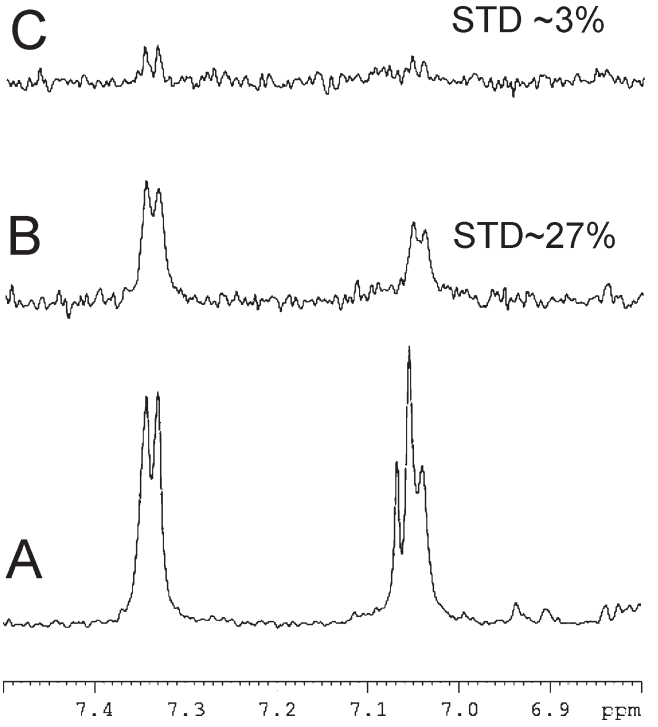

Figure 1. Binding of **3** to AMCase: (A) 1D reference NMR spectrum of aromatic protons of **3** (100 μM); (B) STD spectrum of aromatic protons of **3** (100 μM) with AMCase protein (7 μM); (C) STD competition spectrum of aromatic protons of **3** (100 μM) with AMCase protein (7 μM) and methylallosamidin (20 μM).

Table 1. Comparison of Hit Rates for Different Methods of Hit Identification

methods[a]	HTS	VS	FBS
no. of compounds screened	446K	150K	1045
no. of primary hits (hit rate %)	5257 (1.18%)	918	15 (1.43%)
no. of confirmed hits (hit rate %)	825 (0.18%)	18 (1.96%)	10 (0.96%)

[a] HTS primary hit: molecule with $>14\%$ apparent inhibition at 10 μM concentration in AMCase enzyme assay; HTS confirmed hit: primary hit with $>14\%$ inhibition in confirmation at 10 μM concentration in AMCase enzyme assay; VS primary hit: molecule which docks into enzyme active site in crystal structure; VS confirmed hit: VS hit with $>14\%$ apparent inhibition at 50 μM concentration in AMCase enzyme assay; FBS primary hit: molecule which shows $>4\%$ STD signal in NMR binding experiment; FBS confirmed hit: FBS hit which showed significant reduction in STD signal when allosamidin was added.

or virtual libraries of millions of molecules to be screened rapidly. With tiered-scoring protocols a simple, often shaped-based scoring function acts as a fast initial filter and then progressively more rigorous and computationally intensive methods are applied to the top hits to produce the final ranked list of molecules for experimental testing.

A library of approximately 150000 lead-like compounds (MW $<$ 400) was virtually screened for compound structures that docked to the AMCase protein structure.[10] A total of 918 compounds identified in silico were assayed for AMCase inhibition. This resulted in identification of 18 compounds which were inhibitory at 50 μM, of which 8 compounds had IC_{50} values ranging from 7 to 110 μM, and the most potent compound **1** ($IC_{50} = 210$ nM), which was also identified in the HTS. The hit rates obtained with HTS, VS, and FBS approaches are

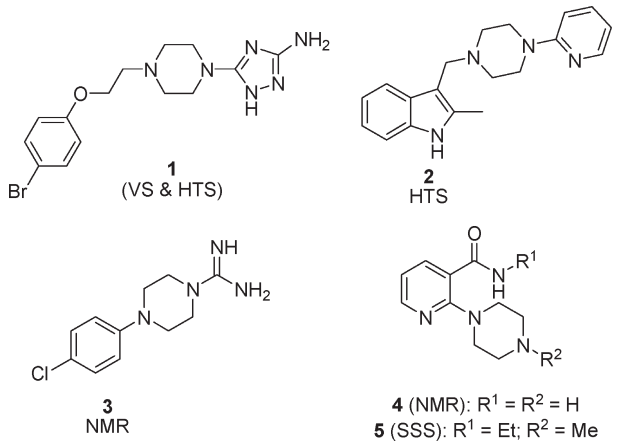

Figure 2. Structures of AMCase inhibitors identified by HTS, FBS, VS, and substructure search (SSS).

summarized in Table 1, and show that while the hit rate was highest with the VS, the number of hits obtained was higher with the HTS because more compounds were tested.

A Biacore-based binding assay was used to characterize the 15 hits identified by NMR-FBS, along with a set of 9 compounds which did not show binding in the NMR screen, as negative controls, and the HTS/VS hit **1** as a positive control. Four of the 15 fragments and **1** showed reproducible binding (>5 RU), while 11 fragments and the 9 negative controls did not show binding (<5 RU) (Figure 3A). The four fragments bound reproducibly and showed the expected 1:1 stoichiometry in three independent AMCase sensor chip surfaces (Figure 3B). In steady state K_D determinations, two of the fragments were too weak to get an accurate fit from the steady state binding (data not shown). The other two fragments (**3** and **4**, Figure 2) and the HTS/VS compound (**1**) each showed concentration dependent binding as expected and quickly reached steady state (Figure 4A). The HTS/VS hit **1** had 10- and 88-fold lower K_D compared to the fragments **3** and **4**, respectively (Figure 4B). In general, there is good correlation between the binding affinities and the IC_{50} values (Table 2).

The hits sets from HTS, FBS, and VS were combined and the calculated properties analyzed (Figure 5). By design, the FBS hits have lower MW and clogP, therefore even though they are weaker inhibitors (IC_{50} up to 500 μM), many have comparable LE and LLE to the HTS hits ($IC_{50} < 0.1-100$ μM), suggesting that they may be equally good starting points for optimization.

Co-crystallization was successfully used to characterize several high affinity hits. AMCase crystals also grew readily in the presence of a weak 124 μM affinity binder, and these crystals were amenable to soaking by virtue of the crystal packing and the low affinity of the ligand. This soaking method was used to obtain costructures with many further inhibitors identified by HTS and other methods. The AMCase cocrystal complex with the high affinity HTS/VS hit **1** was determined to 1.9 Å resolution, using the apo AMCase structure[10] as a search model for molecular replacement. Similar to the previously determined structure of AMCase with the inhibitor methylallosamidin,[10] the aminotriazole moiety of **1** binds in the active site, packing between Trp-360 and Met-210, with H-bonds to Asp-138, Glu-140, and Tyr-212 (Figure 6). However, in contrast to methylallosamidin, the structure reveals that the bromobenzene moiety of **1**

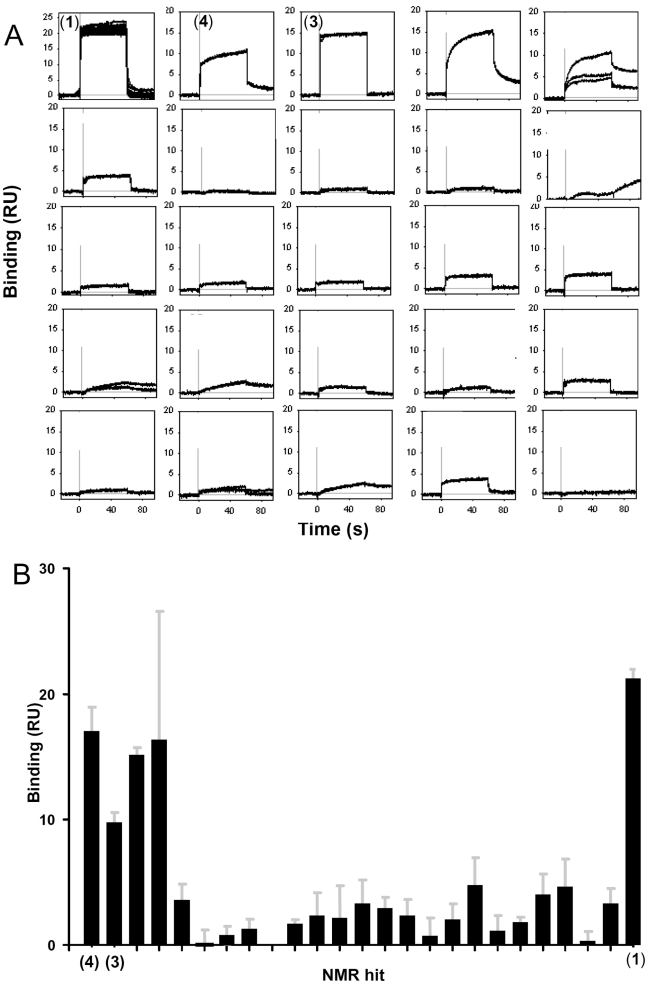

Figure 3. Binding of FBS hits to AMCase by SPR. (A) Response units monitored in real time for a single concentration of each fragment (250 μM) to an AMCase sensor chip surface. (B) Response units from steady state binding of fragments at 250 μM to an AMCase sensor chip surface. Each bar represents the mean and standard deviation of all data obtained from three independent experiments, each done in triplicate.

also exploits a nearby hydrophobic pocket formed by the side chains of Tyr-267, Ala-295, Ile-300, and Leu-364 while the methylallosamidin binds along the chitin binding groove, with an acetyl group only superficially approaching this hydrophobic pocket. Compound **2** binds very similarly to **1** with the pyridine ring occupying the Trp-360/Met-210 active site and the piperazine moiety overlaying with that of **1**. The indole ring extends into the Tyr-267/Ala-295/Ile-300/Leu-364 hydrophobic pocket (Figure 8).

Attempts to cocrystallize the weaker FBS hits in many cases yielded only crystals of apo protein. However, several of the more potent compounds including **3** and the substructure search analogue **5** were successfully cocrystallized. Subsequent trials to introduce other FBS hits by soaking experiments were similarly unsuccessful. Although both **3** and **5** contain an aryl piperazine moiety, the two fragments have very different binding modes and occupy different binding pockets (Figure 7). The predominant feature of the binding mode of **3** is the occupation of the Tyr-267/Ala-295/Ile-300/Leu-364 hydrophobic pocket by the *para*-chlorophenyl group, with the piperazine N forming an H-bond with Asp-213 while the guanidinium group makes H-bonds to

Table 2. AMCase Inhibitors: Calculated Properties, Binding, and IC_{50}

hit	hit source	MW	clogP	LE[a]	LLE[a]	NMR STD% and with competition[a]	AMCase IC_{50} (μM)	chitotriosidase IC_{50} (μM)	Biacore K_D (μM)
1	VS/HTS	367	3	0.42	3.7	6 to 0	0.21	4.23	1.69
2	HTS	306	3.4	0.37	2.8	22 to 4	0.7	1.34	
3	NMR	239	1.8	0.43	3.1	27 to 3	13	> 100	17
4	NMR	206	−0.2	0.37	4.2	ND	101.7	90.1	141
5	SSS	248	1.1	0.36	3.6	ND	22		

[a] LE = $-1.4 \times \log(IC_{50})$/heavy atoms; LLE = $-\log(IC_{50})$ − clogP: NMR % STD signal with and without competitor.

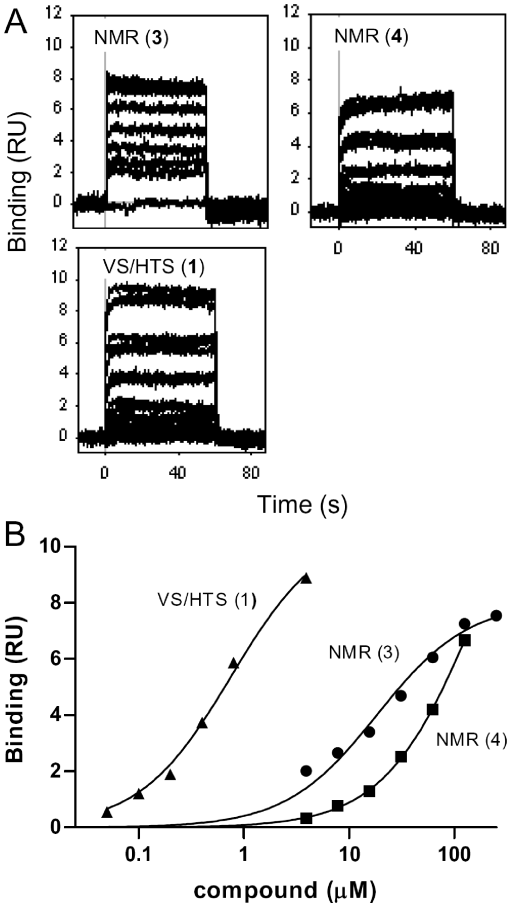

Figure 4. Steady state binding to AMCase. (A) Response units monitored in real time for a concentration series of fragments identified by NMR (**3** and **4**) and VS/HTS (**1**) to an AMCase sensor chip surface. (B) Response units from steady state binding of compounds to an AMCase sensor chip surface. Data were fit to a 1:1 saturation binding model for K_D determination.

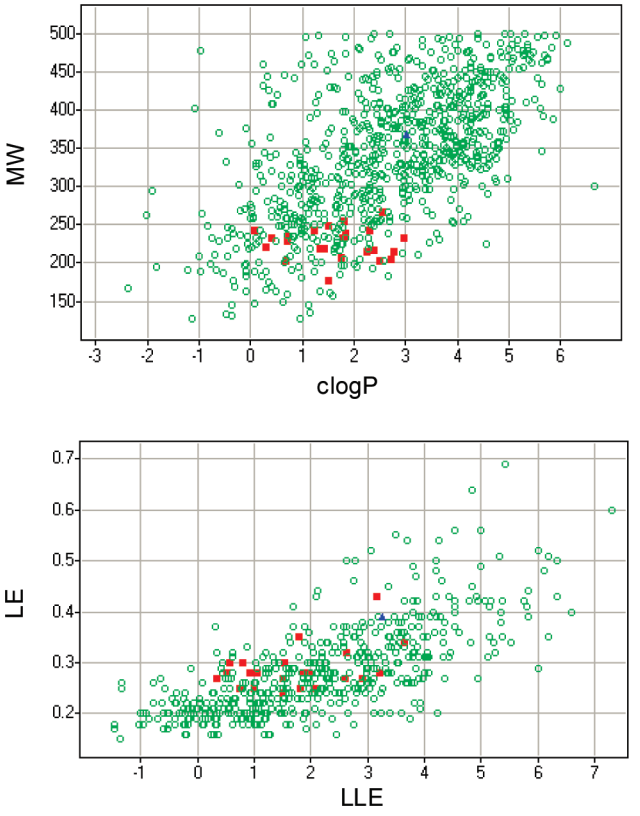

Figure 5. Properties of hits identified by HTS (green open circles), FBS (red filled squares), and VS (blue filled triangles). LE = ΔG/number of heavy atoms (non-H atoms, HA) = $-1.4 \log IC_{50}$/HA; LLE = $-\log IC_{50}$ − clogP.[14]

the Glu-140 side chain. In contrast, the pyridine moiety of **5** packs between Trp-360 and Met-210 in the active site with the piperazine overlapping minimally with that of **3** and forming the same H-bond with Asp-213. The amide moiety reaches out on the bottom face of the pocket making an H-bond with the backbone NH of Trp-99.

It is interesting that the two fragments **3** and **5** identified almost mutually exclusive pockets, both of which appear to be very important for high affinity binding of the larger more potent HTS hits **1** and **2** (Figure 6−8). In fact, the binding pocket and many of the H-bonds made by the higher affinity inhibitors **1** and **2** and are simply the sum of the interactions of the two lower affinity fragments **3** and **5**. This offers support for the concept of linking fragments as a valid path forward to achieving higher potency compounds.

One goal of developing small molecule inhibitors for AMCase is for use in in vivo models of allergic airway disease in order to more fully understand the role of AMCase, which is highly up-regulated in several allergen-challenged models.[3,5,28] In the present study, mice sensitized and challenged with a combination of the house dust mite and cockroach allergens (HDM/CRA) showed an increase in chitinase activity in bronchoalveolar lavage (BAL) fluid compared to PBS challenged animals (Figure 9). In vivo dosing of the potent and selective AMCase inhibitor **1** led to a significant (43%) reduction in the chitinase activity present in BAL fluid taken 1 day after the last day of allergen challenge. The positive control for this allergen model, the corticosterioid dexamethasone, also resulted in reduced chitinase activity (60% reduction) in BAL fluid, as expected, due to reduced chitinase production as previously reported.[29] This orally active AMCase inhibitor **1** should prove a valuable tool compound in further elucidating the role of AMCase in allergic responses.

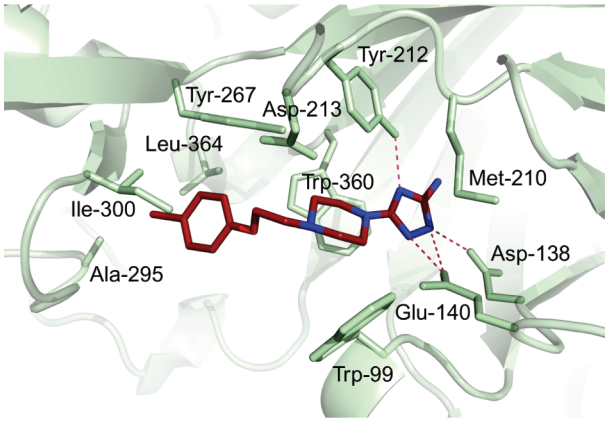

Figure 6. AMCase costructure with **1**. Ribbons diagram of the active site region with selected side chains shown as sticks. Hydrogen bonds are shown as dotted lines.

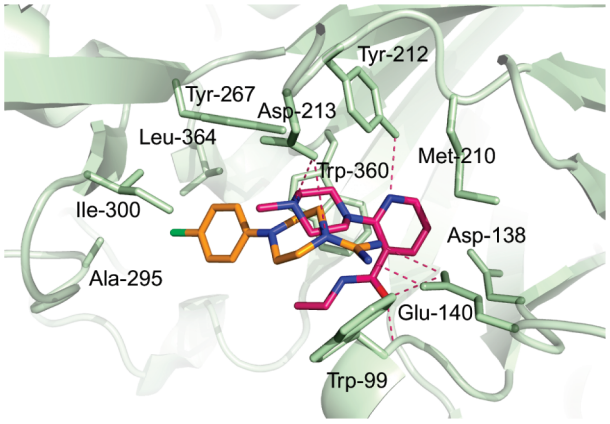

Figure 7. Superposition of independent AMCase costructures with **3** (orange) and **5** (pink). Ribbons diagram and selected side chain sticks are shown for the active site area and hydrogen bonds are shown as dashed lines.

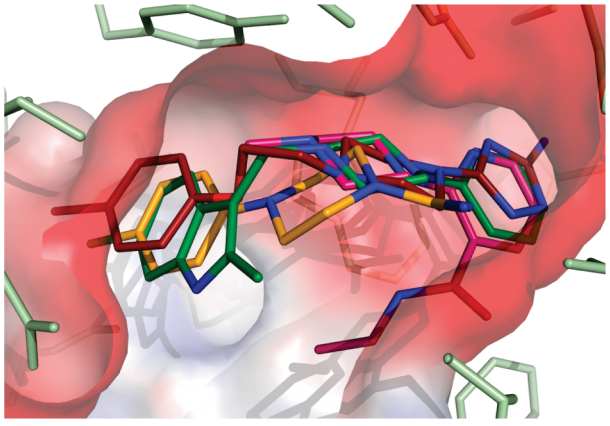

Figure 8. Comparison of compound binding modes based on a superposition of α-carbon backbones of AMCase costructures with **1** (red), **2** (green), **3** (orange), and **5** (pink), and the protein surface colored by electrostatic surface potential. The aromatic rings of **1** (4-bromophenyl) and **2** (indole) overlay well with fragment **3** (4-chloro-phenyl), and the piperazine and heteroaryl ring at the other end of **1** (triazine) and **2** (pyridine) overlap well with fragment **5** (pyridine).

Conclusions

We employed HTS, FBS, and VS strategies to identify novel AMCase inhibitors. Each approach has pros and cons and yielded somewhat overlapping, yet complementary results. This multipronged approach may be advantageous in obtaining a thorough understanding of the possibilities available in the inhibition of the enzyme at the outset, before a large investment into synthetic chemistry optimization efforts. A comparison of the X-ray structures of the fragments bound to AMCase with the structure of the HTS and VS hits helps to illustrate the potential power of fragment-based screening. Small hits identified by screening approximately 1000 fragments were found to occupy two almost mutually exclusive pockets. An overlay of these fragments with the larger hits obtained by screening almost a half million compounds show how occupation of these two pockets appears to be required for higher affinity inhibition. This suggests possibilities for linking the fragments to increase binding affinity. The virtual screening of 150K compounds prioritized about 1000 compounds for testing and led to the identification of one of the more potent hits also identified by the HTS. This potent, selective AMCase inhibitor **1** was characterized and shown to be orally active in reduction of AMCase activity in the BAL fluid of allergen challenged mice.

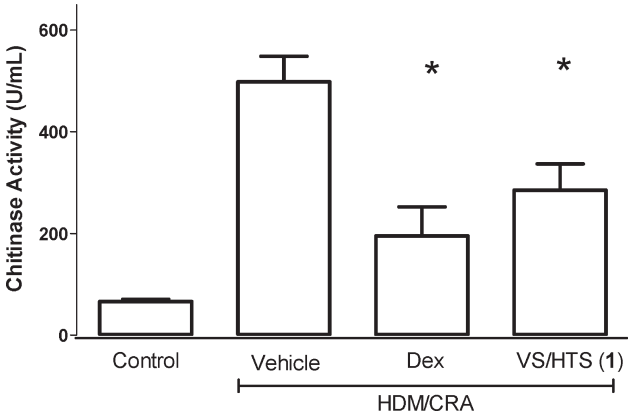

Figure 9. AMCase inhibitors attenuate chitinase activity in allergen-challenged mice. Chitinase activity from bronchoalveolar lavage recovered from mice sensitized with HDM/CRA allergens and challenged with either PBS marked as control, HDM/CRA, or HDM-CRA plus VS/HTS **1**, as indicated. n = at least 10 for each group. * = $p < .01$ compared to allergen challenged.

Experimental Section

Unless otherwise specified, standard laboratory reagents were purchased from Sigma, Aldrich, Research Organics, or EMD. Recombinant human AMCase and methylallosamidin purified from Streptomyces were used as previously described.[10]

AMCase Inhibitors. Inhibitors were either purchased from commercial suppliers, i.e., **2** (Maybridge Screening Collection, part no. HTS06499SC), **3** and **4** (Aurora Screening Library, part no. kchi-774947 and bb-kuk-028119), or synthesized following literature procedures, i.e., **1**[30] and **5**.[31] All compounds had ≥95% purity as measured by two HPLC methods.

AMCase HTS Assay Conditions. The assay conditions for HTS, 15 μM 4-methylumbelliferyl-β-D-*N*,*N*′-diacetylchitobioside substrate (Sigma, St. Louis, MO), 1.5 nM enzyme, 1% DMSO, 30 μL/well) have a *Z*-factor of 0.67 and signal-to-noise of 11.3 at 90 min read time. Fluorescence intensity was monitored at λ excitation 340/20, emission 480/20. A counter screen was performed with 10 μM compound and 2 μM of the product, 4-methylumbelliferone sodium salt (Sigma) in the same buffer and fluorescence intensity wavelengths at the enzyme assay described above.

AMCase and Chitotriosidase Assays. In experiments subsequent to the HTS, chitinolytic activity was measured as previously described.[9] Briefly, AMCase (1 nM) or chitotriosidase

(0.25 nM) were incubated with various concentrations of compounds plus 20 μM 4-methylumbelliferyl β-*N*,*N*′-diacetylchitobioside (Sigma). Fluorescence intensity (λ excitation 345/5, emission 440/5) was monitored for 60 min. Assays were performed in triplicate at 25 °C in 100 mM citrate phosphate buffer pH 5.0, 0.005% Brij-35. The IC_{50} values were derived from eq 1.

$$Y = 100/\left(1+10^{(X-\text{Log IC}_{50})}\right) \quad (1)$$

BAL fluid samples were diluted 1:20 with 20 μM 4-methylumbelliferyl β-*N*,*N*′-diacetylchitobioside substrate (Sigma) and monitored for 30 min at the same wavelengths as described above. The relative chitinase activity units were determined from the slope of activity measured from the linear portions of the enzyme assay.

Virtual Screen. The AMCase/methylallosamidin X-ray complex structure[10] with the ligand and waters removed was screened using the in-house docking program, PhDock.[32−34] Ten poses each for the top 2000 hits based on the DOCK4 contact score[35] were rescored using an molecular mechanics−Poisson−Boltzmann surface area (MM-PBSA) procedure[36,37] and after visual inspection compounds were selected for experimental testing.

NMR FBS Screen. Library collection and NMR samples: The NMR fragment library composed of 1045 compounds was selected from the corporate library based on a combination of calculated property criteria, (MW < 300, clogP < 3, H-bond donors < 3, H-bond acceptors < 4, rotatable bonds < 3, polar surface area < 120 Å^2 and chiral centers < 1), medicinal chemist prioritization, and amenability to being chemically modified. DMSO stocks solutions of the compounds (80 mM) were diluted to 25 mM in TRIS buffer at pH = 7.4 containing 50 mM NaCl and a final concentration of 5% DMSO for NMR. Compounds were screened for binding to AMCase (5 μM) as mixtures of six, with each compound at 200 μM. All spectra were acquired at 298K with a Bruker Avance 600 MHz NMR spectrometer, equipped with a cryogenic probe and autosampler. Screening was performed with the saturation transfer difference (STD)[38] experiment, where the protein was saturated on resonance at 0.58 ppm and off resonance at −10 ppm, for 2 s each, using a train of 40 G4 Gian pulses of 50 ms between 1 ms delays. The subtraction of the STD spectra was performed internally with phase cycling. The relaxation delay was 2 s. Mixtures which demonstrated binding were deconvoluted by conducting binding experiments on individual compounds, followed by methylallosamidin competition experiments.

Surface Plasmon Resonance Binding Experiments. Sensor chip surfaces were prepared on a Biacore T100 instrument (Biacore Inc., Piscataway, NJ), using reagents obtained from the manufacturer. AMCase was biotinylated by mixing a 4:1 ratio of biotin (Invitrogen, Eugene OR) to AMCase for 30 min and then removing the unreactive biotin by extensive dialysis. The biotinylated AMCase was injected onto a SA chip reaching surface densities between 4000 and 6000 RU. Measurements were performed at 25 °C, 100 μL per min, and a collection rate of 10 Hz. Various concentrations of compounds were prepared in 100 mM citrate phosphate buffer with 0.05% Tween 20 and a final DMSO concentration of 1%. For direct measurements of compounds, 250 μM were injected over the AMCase sensor chip surface. All injections were performed in triplicate. The experimental data were corrected for instrumental and bulk artifacts by double referencing a control sensor chip surface and buffer injections using Scrubber software (BioLogic Software v1.1 g).[39] A DMSO calibration curve was applied as previously described.[40] Steady-state binding derived from the transformed data was used to determine compound affinity using BiaEvaluation v4.1 (GE Healthcare, Piscataway NJ).

Crystallization. AMCase was cocrystallized in complex with **1** by hanging drop vapor diffusion at 18 °C in drops containing 0.2 μL of protein solution (0.44 mM AMCase, 0.52 mM **1**, 25 mM Tris-HCl pH 8.0, and 50 mM NaCl) mixed with 0.2 μL of well solution (20% PEG MME 5000, 100 mM bis-tris pH 6.5) and equilibrated against 200 μL of well solution. Slate-like crystals grew in two weeks.

NMR hits were pursued with a combination of targeted screening and broad screening. Targeted screening was done by hanging drop vapor diffusion at 18 °C in drops containing 1 μL of protein solution (0.44 mM AMCase, 5 mM compound of interest diluted from a 100 mM DMSO stock, 25 mM Tris-HCl pH 8.0, and 50 mM NaCl) mixed with 1 μL of well solution (20% PEG 3350, 200 mM magnesium formate) and equilibrated against 500 μL of well solution. Crystals were obtained for **3** and **5**. Broad screening was done by hanging drop vapor diffusion at 18 °C in drops containing 0.2 μL of protein solution (0.44 mM AMCase, 5 mM compound of interest diluted from a 100 mM DMSO stock, 25 mM Tris-HCl pH 8.0, and 50 mM NaCl) mixed with 0.2 μL of well solution and equilibrated against 200 μL of well solution where the well solution was commercially available PEG/ion based screens. Several other fragments also produced crystals which were subsequently determined to be apo AMCase crystals.

Soaking experiments were carried out with crystals grown in the presence of a weak binder (AY-26439) and crystallized by vapor diffusion against 20% PEG 3350, 100 mM bis-tris pH 6.5. These crystals were transferred to 10 μL of a soaking buffer composed of 23% PEG3350, 100 mM bis-tris pH 6.5, 5 mM compound of interest, 5% DMSO.

Data collection and processing: Crystals were drawn through a solution of 25% glycerol and 75% well solution and cooled rapidly in liquid nitrogen. Diffraction data were recorded at ALS beamline 5.0.1 on a q-210 ccd camera. Intensities were integrated and scaled using the programs Denzo and Scalepack.[41]

Phasing, model building and refinement: Structures were determined by molecular replacement using the protein model of the human chitotriosidase in complex with methylallosamidin (PDB ID = 3FY1) as the search model. The final structure models were obtained after several iterative cycles of refinement using CNX[42] and Refmac5[43] and model improvement in Coot.[44]

HDM-CRA Mouse Model of Allergic Pulmonary Inflammation. All in vivo experiments were performed in accordance with protocols approved by Wyeth's Institutional Animal Care and Use Committee. Age-matched 6−8-week-old female C57BL6 mice (Taconic, Hudson, NY) were sensitized intraperitoneally with a combination of 40 μg of American cockroach extract (CRA; *Periplaneta americana;* Greer, Lenoir, NC) and 40 μg house dust mite extract (HDM; Der p; *Dermatophagoides pteronyssinus;* Greer, Lenoir, NC) emulsified in 4 mg alum (ImjectAlum; Pierce, Rockford, IL) on days 0 and 7. Starting on day 14, mice were challenged intranasally (IN) with either 50 μL pf PBS or 25 μg (50 μL) of HDM/CRA (12.5 μg HDM extract and 12.5 μg CRA extract). This was repeated for 2 d. Test articles were dissolved in 0.5% methylcellulose and 2% Tween 80, administered orally at 50 mg/kg twice daily on the day prior to allergen challenge and again 2 h prior to challenge and 8 h after challenge. Dexamethasone (Dex; 10 mg/kg) was administered intraperitoneally once daily prior to allergen challenge. The mice were allowed to rest for a day, and on day 17 animals were euthanized by carbon dioxide asphyxiation and bronchoalveolar lavage (BAL) fluid was collected by lavaging the lung once with 0.7 mL PBS-CMF. The BAL fluid was stored at −80 °C prior to measurement of the chitinolytic activity in these samples as described above.

Supporting Information Available: HPLC purity of compounds. This material is available free of charge via the Internet at http://pubs.acs.org.

References

(1) Holgate, S. T. Pathogenesis of asthma. *Clin. Exp. Allergy* **2008**, *38*, 872–897.
(2) van Aalten, D. M.; Komander, D.; Synstad, B.; Gaseidnes, S.; Peter, M. G.; Eijsink, V. G. Structural insights into the catalytic mechanism of a family 18 exo-Chitinase. *Proc. Natl. Acad. Sci. U.S.A* **2001**, *98*, 8979–8984.

(3) Zhu, Z.; Zheng, T.; Homer, R. J.; Kim, Y. K.; Chen, N. Y.; Cohn, L.; Hamid, Q.; Elias, J. A. Acidic mammalian chitinase in asthmatic Th2 inflammation and IL-13 pathway activation. *Science* **2004**, *304*, 1678–1682.
(4) Homer, R. J.; Zhu, Z.; Cohn, L.; Lee, C. G.; White, W. I.; Chen, S.; Elias, J. A. Differential expression of chitinases identify subsets of murine airway epithelial cells in allergic inflammation. *Am. J. Physiol. Lung. Cell Mol. Physiol.* **2006**, *291*, L502–L511.
(5) Follettie, M. T.; Ellis, D. K.; Donaldson, D. D.; Hill, A. A.; Diesl, V.; DeClercq, C.; Sypek, J. P.; Dorner, A. J.; Wills-Karp, M. Gene expression analysis in a murine model of allergic asthma reveals overlapping disease and therapy dependent pathways in the lung. *Pharmacogenomics J.* **2006**, *6*, 141–152.
(6) Rao, F. V.; Houston, D. R.; Boot, R. G.; Aerts, J. M.; Sakuda, S.; van Aalten, D. M. Crystal structures of allosamidin derivatives in complex with human macrophage chitinase. *J. Biol. Chem.* **2003**, *278*, 20110–20116.
(7) Sakuda, S.; Isogai, A.; Matsumoto, S.; Suzuki, A. Search for microbial insect growth regulators. II. Allosamidin, a novel insect chitinase inhibitor. *J. Antibiot.* (*Tokyo*) **1987**, *40*, 296–300.
(8) Reese, T. A.; Liang, H. E.; Tager, A. M.; Luster, A. D.; Van Rooijen, N.; Voehringer, D.; Locksley, R. M. Chitin induces accumulation in tissue of innate immune cells associated with allergy. *Nature* **2007**, *447*, 92–96.
(9) Chou, Y. T.; Yao, S.; Czerwinski, R.; Fleming, M.; Krykbaev, R.; Xuan, D.; Zhou, H.; Brooks, J.; Fitz, L.; Strand, J.; Presman, E.; Lin, L.; Aulabaugh, A.; Huang, X. Kinetic characterization of recombinant human acidic mammalian chitinase. *Biochemistry* **2006**, *45*, 4444–4454.
(10) Olland, A. M.; Strand, J.; Presman, E.; Czerwinski, R.; Joseph-McCarthy, D.; Krykbaev, R.; Schlingmann, G.; Chopra, R.; Lin, L.; Fleming, M.; Kriz, R.; Stahl, M.; Somers, W.; Fitz, L.; Mosyak, L. Triad of polar residues implicated in pH specificity of acidic mammalian Chitinase. *Protein Sci.* **2009**, *18*, 569–578.
(11) Fox, S.; Farr-Jones, S.; Sopchak, L.; Boggs, A.; Comley, J. High-throughput screening: searching for higher productivity. *J. Biomol. Screening* **2004**, *9*, 354–358.
(12) Fox, S.; Farr-Jones, S.; Sopchak, L.; Boggs, A.; Nicely, H. W.; Khoury, R.; Biros, M. High-throughput screening: update on practices and success. *J. Biomol. Screening* **2006**, *11*, 864–869.
(13) Keseru, G. M.; Makara, G. M. The influence of lead discovery strategies on the properties of drug candidates. *Nature Rev. Drug Discovery* **2009**, *8*, 203–212.
(14) Leeson, P. D.; Springthorpe, B. The influence of drug-like concepts on decision-making in medicinal chemistry. *Nature Rev. Drug Discovery* **2007**, *6*, 881–890.
(15) Hajduk, P. J.; Greer, J. A decade of fragment-based drug design: strategic advances and lessons learned. *Nature Rev. Drug Discovery* **2007**, *6*, 211–219.
(16) Congreve, M.; Chessari, G.; Tisi, D.; Woodhead, A. J. Recent developments in fragment-based drug discovery. *J. Med. Chem.* **2008**, *51*, 3661–3680.
(17) Fink, T.; Bruggesser, H.; Reymond, J. L. Virtual exploration of the small-molecule chemical universe below 160 Da. *Angew. Chem., Int. Ed. Engl.* **2005**, *44*, 1504–1508.
(18) Hann, M. M.; Oprea, T. I. Pursuing the leadlikeness concept in pharmaceutical research. *Curr. Opin. Chem. Biol.* **2004**, *8*, 255–263.
(19) Rees, D. C.; Congreve, M.; Murray, C. W.; Carr, R. Fragment-based lead discovery. *Nature Rev. Drug Discovery* **2004**, *3*, 660–672.
(20) Wyss, D.; Eaton, H. L. Fragment-Based Approaches to Lead Discovery. *Front. Drug Des. Discovery* **2007**, *3*, 171–202.
(21) Schade, M. NMR fragment screening: Advantages and applications. *IDrugs* **2006**, *9*, 110–113.
(22) Neumann, T.; Junker, H. D.; Schmidt, K.; Sekul, R. SPR-based fragment screening: advantages and applications. *Curr. Top. Med. Chem.* **2007**, *7*, 1630–1642.
(23) Perspicace, S.; Banner, D.; Benz, J.; Muller, F.; Schlatter, D.; Huber, W. Fragment-based screening using surface plasmon resonance technology. *J. Biomol. Screening* **2009**, *14*, 337–349.
(24) Ockey, D. A.; Dotson, J. L.; Struble, M. E.; Stults, J. T.; Bourell, J. H.; Clark, K. R.; Gadek, T. R. Structure−activity relationships by mass spectrometry: identification of novel MMP-3 inhibitors. *Bioorg. Med. Chem.* **2004**, *12*, 37–44.
(25) Nienaber, V. L.; Richardson, P. L.; Klighofer, V.; Bouska, J. J.; Giranda, V. L.; Greer, J. Discovering novel ligands for macromolecules using X-ray crystallographic screening. *Nature Biotechnol.* **2000**, *18*, 1105–1108.
(26) Muegge, I. Synergies of virtual screening approaches. *Mini-Rev. Med. Chem.* **2008**, *8*, 927–933.
(27) Joseph-McCarthy, D.; Baber, J. C.; Feyfant, E.; Thompson, D. C.; Humblet, C. Lead optimization via high-throughput molecular docking. *Curr. Opin. Drug Discovery Dev.* **2007**, *10*, 264–274.
(28) Nair, M. G.; Gallagher, I. J.; Taylor, M. D.; Loke, P.; Coulson, P. S.; Wilson, R. A.; Maizels, R. M.; Allen, J. E. Chitinase and Fizz family members are a generalized feature of nematode infection with selective upregulation of Ym1 and Fizz1 by antigen-presenting cells. *Infect. Immun.* **2005**, *73*, 385–394.
(29) Zhao, J.; Yeong, L. H.; Wong, W. S. Dexamethasone alters bronchoalveolar lavage fluid proteome in a mouse asthma model. *Int. Arch. Allergy Immunol.* **2007**, *142* (3), 219–229.
(30) Tomcufcik, A. S.; Meyer, W. E.; Dusza, J. P. 2-(Substituted-1-piperazinyl)-[1,2,4]triazolo[1,5-*a*]pyrimidines. U.S. Patent 4,582,833, 1986.
(31) Thunus, L.; Lapiere, C. L. 3-Disubstituted 2-(4-methyl-1-piperazinyl)pyridines. *Eur. J. Med. Chem.* **1974**, *9*, 55–58.
(32) Joseph-McCarthy, D.; Thomas, B. E. t.; Belmarsh, M.; Moustakas, D.; Alvarez, J. C. Pharmacophore-based molecular docking to account for ligand flexibility. *Proteins* **2003**, *51*, 172–188.
(33) Joseph-McCarthy, D.; Alvarez, J. C. Automated generation of MCSS-derived pharmacophoric DOCK site points for searching multiconformation databases. *Proteins* **2003**, *51*, 189–202.
(34) Joseph-McCarthy, D. M., I. J.; Zou, J.; Walker, G.; Alvarez, J. C. *Pharmacophore-Based Molecular Docking: A Practical Guide*; Marcel Dekker: New York, 2005; pp 327−347.
(35) Ewing, T. J.; Makino, S.; Skillman, A. G.; Kuntz, I. D. DOCK 4.0: search strategies for automated molecular docking of flexible molecule databases. *J. Comput.-Aided Mol. Des.* **2001**, *15*, 411–428.
(36) Rush, T.; I., E.S. Manas, Tawa, G.J.; Alvarez, J.C. *Solvation-Based Scoring for High Throughput Docking*; Marcel Dekker: New York, 2005; pp 249−278.
(37) Thompson, D. C.; Humblet, C.; Joseph-McCarthy, D. Investigation of MM-PBSA rescoring of docking poses. *J. Chem. Inf. Model.* **2008**, *48*, 1081–1091.
(38) Mayer, M.; Meyer, B. Characterization of ligand binding by saturation transfer difference NMR spectroscopy. *Angew. Chem., Int. Ed. Engl.* **1999**, *38*, 1784–1788.
(39) Myszka, D. G. Survey of the 1998 optical biosensor literature. *J. Mol. Recognit.* **1999**, *12*, 390–408.
(40) Frostell-Karlsson, A.; Remaeus, A.; Roos, H.; Andersson, K.; Borg, P.; Hamalainen, M.; Karlsson, R. Biosensor analysis of the interaction between immobilized human serum albumin and drug compounds for prediction of human serum albumin binding levels. *J. Med. Chem.* **2000**, *43*, 1986–1992.
(41) Otwinowski, Z.; Minor, W. Processing of X-ray Diffraction Data Collected in Oscillation Mode. *Methods Enzymol.* **1997**, *276*, 307–326.
(42) Brunger, A. T.; Adams, P. D.; Clore, G. M.; DeLano, W. L.; Gros, P.; Grosse-Kunstleve, R. W.; Jiang, J. S.; Kuszewski, J.; Nilges, M.; Pannu, N. S.; Read, R. J.; Rice, L. M.; Simonson, T.; Warren, G. L. Crystallography & NMR system: aA new software suite for macromolecular structure determination. *Acta. Crystallogr., Sect. D: Biol. Crystallogr.* **1998**, *54*, 905–921.
(43) CCP4. The CCP4 suite: programs for protein crystallography. *Acta. Crystallogr., Sect. D: Biol. Crystallogr.* **1994**, *50*, 760–763.
(44) Emsley, P.; Cowtan, K. Coot: model-building tools for molecular graphics. *Acta. Crystallogr., Sect. D: Biol. Crystallogr.* **2004**, *60*, 2126–2132.